High Power Laser Science and Engineering, (2021), Vol. 9, e50, 5 pages.
doi: 10.1017/hpl.2021.42

HIGH POWER LASER SCIENCE AND ENGINEERING

LETTER

Power-scalable sub-100-fs Tm laser at 2.08 μm

Li Wang[1], Weidong Chen[1], Yongguang Zhao[1,2], Hanlin Yang[3,4], Wei Jing[3], Zhongben Pan[3], Hui Huang[3], Jiachen Liu[4], Ji Eun Bae[5], Fabian Rotermund[5], Pavel Loiko[6], Xavier Mateos[7], Zhengping Wang[8], Xinguang Xu[8], Uwe Griebner[1], and Valentin Petrov[1]

[1] *Max Born Institute for Nonlinear Optics and Short Pulse Spectroscopy, 12489 Berlin, Germany*

[2] *Jiangsu Key Laboratory of Advanced Laser Materials and Devices, School of Physics and Electronic Engineering, Jiangsu Normal University, Xuzhou 221116, China*

[3] *Institute of Chemical Materials, China Academy of Engineering Physics, Mianyang 621900, China*

[4] *Key Laboratory of Advanced Ceramics and Mechanical Technology of Ministry of Education, School of Materials Science and Engineering, Tianjin University, Tianjin 300072, China*

[5] *Department of Physics, Korea Advanced Institute of Science and Technology (KAIST), 34141 Daejeon, Republic of Korea*

[6] *Centre de Recherche sur les Ions, les Matériaux et la Photonique (CIMAP), UMR 6252 CEA-CNRS-ENSICAEN, Université de Caen, 14050 Caen Cedex 4, France*

[7] *Física i Cristal·lografia de Materials i Nanomaterials (FiCMA-FiCNA), Universitat Rovira i Virgili (URV), 43007 Tarragona, Spain*

[8] *State Key Laboratory of Crystal Materials and Institute of Crystal Materials, Shandong University, Jinan 250100, China*

(Received 27 May 2021; revised 12 July 2021; accepted 17 September 2021)

Abstract

We report on a power-scalable sub-100-fs laser in the 2-μm spectral range using a Tm^{3+}-doped 'mixed' $(Lu,Sc)_2O_3$ sesquioxide ceramic as an active medium. Pulses as short as 58 fs at 2076 nm with an average output power of 114 mW at a pulse repetition rate of approximately 82.9 MHz are generated by employing single-walled carbon nanotubes as a saturable absorber. A higher average power of 350 mW at 2075 nm is obtained at the expense of the pulse duration (65 fs). A maximum average power of 486 mW is achieved for a pulse duration of 98 fs and an optical conversion efficiency of 22.3%, representing the highest value ever reported from sub-100-fs mode-locked Tm lasers.

Keywords: 2-μm mode-locked laser; single-walled carbon nanotubes; $Tm:(Lu,Sc)_2O_3$

1. Introduction

Sub-100-fs mode-locked (ML) lasers at approximately 2 μm with average powers exceeding 100 mW are attractive for multiple applications, for example, synchronous pumping of optical parametric oscillators (SPOPOs) operating at wavelengths longer than 5 μm[1], mid-infrared (IR) frequency comb generation[2], as seed sources for chirped pulse amplification (CPA) laser systems and near-degenerate chirped pulse optical parametric amplification (CPOPA)[3], for the generation of high harmonics and soft X-rays[4], transparent materials processing[5].

The attractive thermo-optical and spectroscopic properties of thulium (Tm^{3+})-doped cubic sesquioxide A_2O_3 (where A = Y, Lu, Sc or their combinations) make them ideally suited for generating high-power femtosecond pulses from passively ML solid-state lasers in the 2-μm spectral region. Using a single-layer graphene saturable absorber (SA), an average power of 270 mW with a relatively long pulse duration of 410 fs was achieved from an ML $Tm:Lu_2O_3$ ceramic laser[6]. A semiconductor saturable absorber mirror (SESAM) ML laser generating 750 mW and 382 fs pulses was described in Ref. [7] using the same material. Watt-level average output power was achieved via Kerr-lens mode-locking (KLM) of a $Tm:Sc_2O_3$ crystalline laser at 2115 nm with a pulse duration of 298 fs[8]. Note that in all these studies, the relatively narrow gain bandwidths of the simple sesquioxides did not support sub-100-fs pulse generation.

Correspondence to: Y. Zhao, Max Born Institute for Nonlinear Optics and Short Pulse Spectroscopy, 12489 Berlin, Germany. Email: zhao@mbi-berlin.de

Tm^{3+}-doped 'mixed' sesquioxides $(A,B)_2O_3$ with compositional disorder inducing inhomogeneous broadening of the absorption and gain spectra are obviously advantageous in the sub-100-fs regime at 2 μm[9–11]. Compared with crystalline sesquioxides, transparent ceramics offer more flexibility owing to the less-challenging fabrication process. The latter features size scalability, overcoming temperature limits of the crystal growth (very high crystal melting temperatures, typically ~2400°C–2500°C) and the potential for creating controlled 'mixed' compositions with a specific doping level[12,13]. High-quality, almost pore-free Tm^{3+}-doped 'mixed' polycrystalline sesquioxides, for example $Tm:(Lu,Sc)_2O_3$ and $Tm:(Lu,Y)_2O_3$, are fabricated by the hot isostatic pressing (HIP) sintering method[13,14]. Sub-100-fs ML operation of such a Tm^{3+}-doped 'mixed' ceramic laser was first demonstrated in 2018: 63-fs pulses with an average power of only 34 mW were generated at 2057.2 nm employing a SESAM[15]. Subsequently, shorter pulse durations of 57 fs at 2045 nm and 54 fs at 2048 nm were reported using a single-walled carbon nanotube (SWCNT)-based SA and a SESAM, respectively, with average output power still below 100 mW[16,17]. Figure 1 summarizes the state of the art of sub-100-fs ML solid-state Tm lasers emitting in the 2-μm spectral range[16–22]. An average power of 210 mW was demonstrated in 2019 with an SWCNT-SA ML $Tm:LuYO_3$ ceramic laser[16]. In 2020, a slightly higher power of 222 mW was obtained from a $Tm:Sc_2O_3$ laser using the KLM technique[21], which represents the highest power ever reported from such sub-100-fs ML solid-state Tm lasers. One can recognize that all the average powers higher than 100 mW were obtained by using the above-mentioned sesquioxide materials[16,17,21], and an obvious trade-off between average power and pulse duration can be seen from all these reported results.

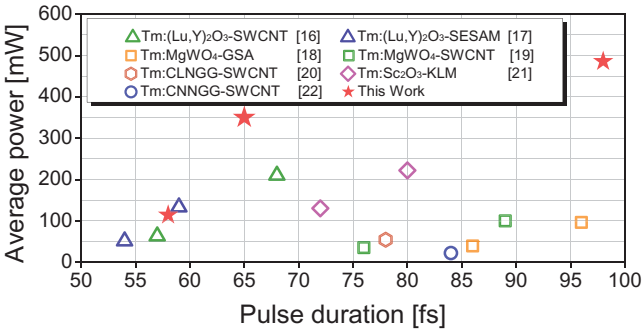

Figure 1. The state-of-the-art of sub-100-fs ML Tm lasers operating in the 2-μm spectral range (average output power versus pulse duration). The red stars summarize our present results.

The above results and the superior thermo-optical and improved spectroscopic properties of the Tm^{3+}-doped 'mixed' polycrystalline sesquioxides motivated us to further explore the feasibility of average power scaling in the sub-100-fs regime. For this purpose, a broadband SA that possesses a low non-saturable loss and high damage threshold at approximately 2 μm is required. Compared with SESAMs, carbon-nanostructure-based SAs, for example graphene[23] and SWCNT SAs[24], exhibit a broader spectral response and are fabricated by simpler and less expensive techniques. Here, we present the performance of a power-scalable SWCNT-SA ML 'mixed' $Tm:(Lu,Sc)_2O_3$ ceramic laser in the sub-100-fs regime at approximately 2.08 μm.

2. Experimental setup

The high-quality 'mixed' $Tm:(Lu_{2/3}Sc_{1/3})_2O_3$ transparent ceramic used in the experiment was fabricated by the HIP sintering method. The Tm^{3+} doping was 2.8% (atomic fraction) ($N_{Tm} = 8.12 \times 10^{20}$ cm^{-3}). A linear X-folded astigmatically compensated resonator was arranged for evaluating the laser performance both in the continuous-wave (CW) and the ML regimes, as illustrated in Figure 2. An uncoated ceramic sample having a thickness of 3 mm and an aperture of 3 mm× 3 mm was mounted on a copper holder with water cooling (coolant temperature: 12°C) and placed between two dichroic folding mirrors, M_1 and M_2 (radius of curvature, RoC = –100 mm), with the Brewster minimum loss condition fulfilled for the laser wavelength. The pump source was a narrow-linewidth CW Ti:sapphire laser tuned to 795 nm emitting linearly polarized radiation. The pump beam was focused into the ceramic using a spherical lens having a focal length of 70 mm to form a waist with beam radii of 30 μm and 77 μm in the sagittal and tangential planes, respectively.

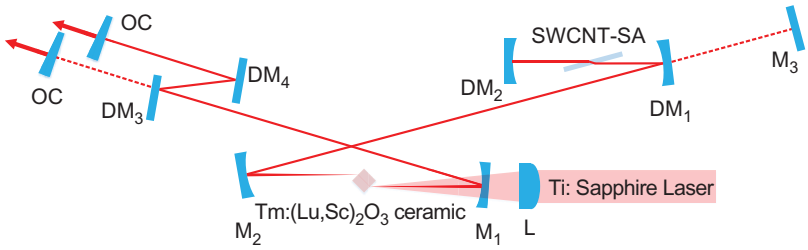

Figure 2. Experimental configuration of the CW and ML $Tm:(Lu,Sc)_2O_3$ ceramic laser. L, focusing lens; M_1 and M_2, concave dichroic mirrors; M_3, plane rear mirror; DM_1–DM_4, dispersive mirrors; OC, output coupler.

3. Results

The CW laser performance was investigated with a four-mirror cavity including a plane rear reflector M_3 and a plane-wedged output coupler (OC; without the SWCNT-SA); see Figure 3(a). The measured single-pass pump absorption under lasing conditions was between 57.4% and 58.6%, depending slightly on the OC (0.2%–3%). A maximum power of 755 mW was obtained at an absorbed power of 1.84 W for the 1.5% OC, corresponding to a slope efficiency of 43.6%. The round-trip passive loss was estimated using the Caird analysis[25], that is, fitting the measured slope efficiency as a function of the OC reflectivity, giving total round-trip resonator losses of $\delta = 0.21\%$, as shown in Figure 3(b). The determined value of δ indicates high optical quality of the transparent ceramic and a well-optimized laser resonator.

To initiate and stabilize a soliton-like ML operation, a transmission-type SWCNT-SA (relying on the first fundamental electronic transition E_{11} of semiconducting nanotubes for absorption at ~2 μm[24]) was employed. The nanotubes were synthesized by the arc-discharge method and the SWCNT/poly(methyl methacrylate) (PMMA) film was spin-coated on a 1-mm-thick fused silica (FS) substrate. The SWCNT-SA exhibited a relatively low non-saturable linear loss of approximately 1%, small saturation fluence of less than 10 μJ/cm^2, very low modulation depth of less than 0.5% and a slow recovery time constant of approximately 1 ps at approximately 2 μm[26]. It was placed at Brewster's angle in the second cavity beam waist having beam radii of 125 μm and 225 μm in the sagittal and tangential planes, respectively. The latter was created by two concave dispersive mirrors (DMs), DM_1 and DM_2, with RoC of –100 and –50 mm, respectively. The steady-state soliton-like pulses were generated by varying the number of bounces on the DMs (DM_1–DM_4) for negative group delay dispersion (GDD) to balance the self-phase modulation (SPM)[27]. All DMs exhibited a GDD of –125 fs^2 per bounce. The roundtrip material GDD due to the 3-mm thick ceramic sample amounted to approximately –200 fs^2 at 2.08 μm, estimated by averaging the refractive indices of Lu_2O_3 and Sc_2O_3[28]. Additional material GDD of approximately –240 fs^2 (per round-trip) was introduced by the FS SA substrate.

In addition to the two concave mirrors DM_1 and DM_2, two bounces on the flat DMs (DM_3 and DM_4) were implemented yielding a net round-trip cavity GDD of –875 fs^2. The ML laser performance was studied by varying the output coupling without changing the cavity length. The latter corresponded to a pulse repetition rate of approximately 82.9 MHz. When applying the 1.5% OC, a self-starting ML operation was achieved with ultimate stability by careful cavity alignment. The central emission wavelength was 2075 nm with a 72 nm FWHM (full width at half maximum). The measured spectrum with its sech^2-shaped fit is shown in Figure 4(a). The recorded fringe-resolved autocorrelation trace leads to a deconvolved pulse duration of 65 fs (FWHM) by assuming a sech^2-shaped temporal profile, as shown in Figure 4(b), which was only 3.4% longer than the Fourier-transform limit. The average output power amounted to 350 mW for an absorbed pump power of 2.2 W corresponding to an optical conversion efficiency η_{opt} of 15.9%. The excellent sech^2-shaped spectral and temporal profiles indicate soliton ML operation of the Tm:$(Lu,Sc)_2O_3$ ceramic laser.

Further power scaling in the ML regime was achieved by increasing the OC transmission at the expense of the pulse

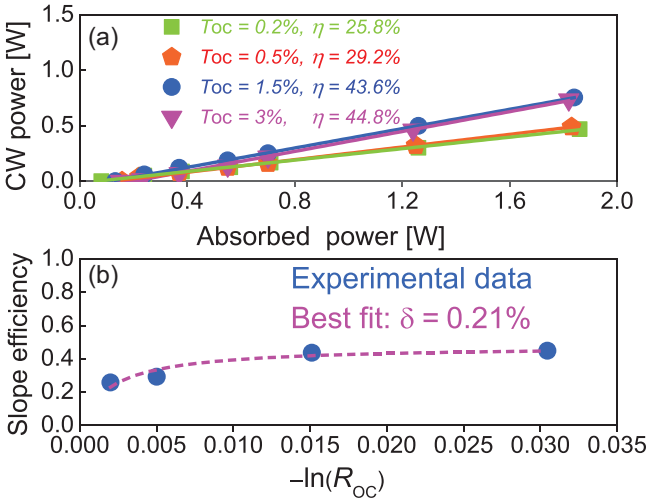

Figure 3. (a) Laser performance of the Tm:$(Lu,Sc)_2O_3$ ceramic laser in the CW regime for different OC transmission T_{OC}. (b) Cavity loss fitting curve with the slope efficiency as a function of the OC reflectivity, $R_{OC} = 1 - T_{OC}$.

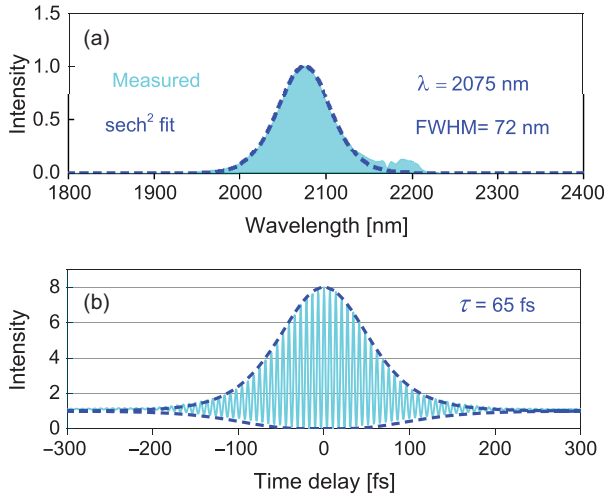

Figure 4. SWCNT-SA ML Tm:$(Lu,Sc)_2O_3$ ceramic laser with $T_{OC} = 1.5\%$: (a) measured optical spectrum and (b) interferometric autocorrelation trace.

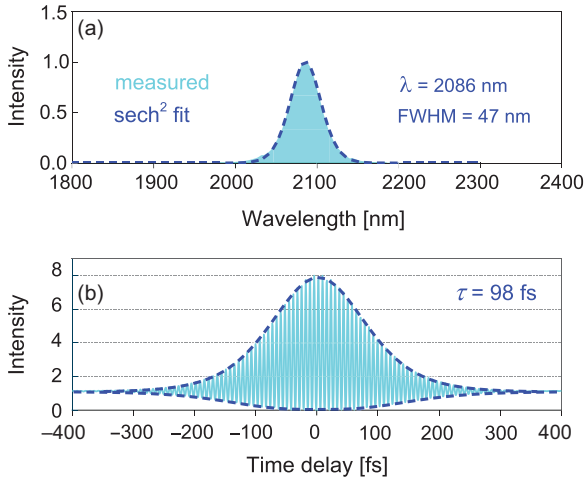

Figure 5. SWCNT-SA ML Tm:$(Lu,Sc)_2O_3$ ceramic laser with $T_{OC} = 3\%$: (a) measured optical spectrum and (b) interferometric autocorrelation trace.

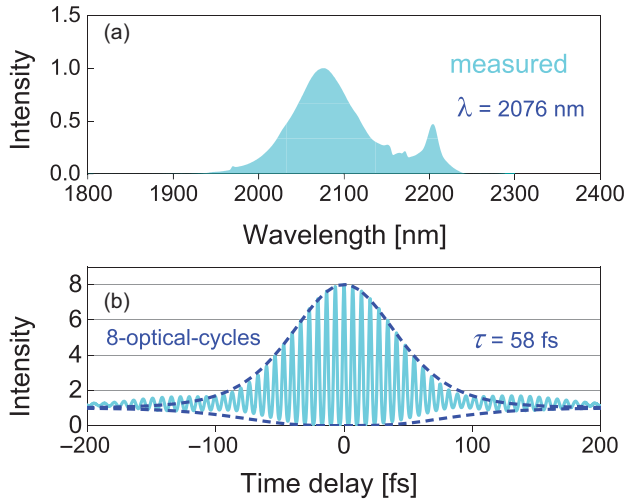

Figure 6. SWCNT-SA ML Tm:$(Lu,Sc)_2O_3$ ceramic laser with $T_{OC} = 0.5\%$: (a) measured optical spectrum and (b) interferometric autocorrelation trace.

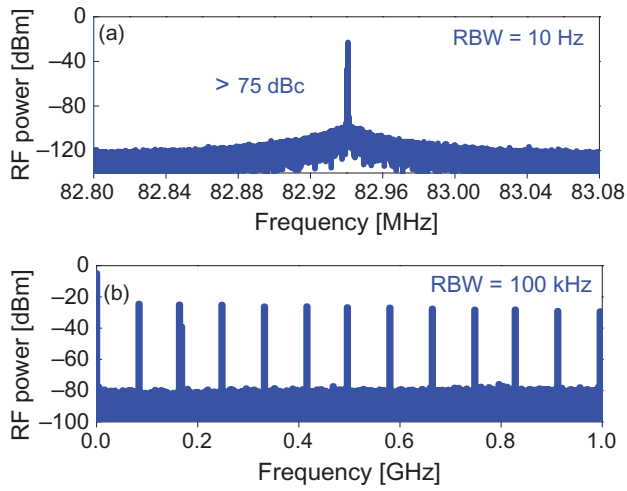

Figure 7. Radio frequency (RF) spectra of the ML Tm:$(Lu,Sc)_2O_3$ ceramic laser with $T_{OC} = 0.5\%$: (a) fundamental beat note and (b) 1-GHz span. RBW, resolution bandwidth.

duration. Indeed, using a 3% OC, the average power reached 486 mW at an absorbed pump power of 2.18 W, which corresponded to $\eta_{opt} = 22.3\%$. Figure 5 shows the measured spectrum and fringe-resolved autocorrelation trace. The pulses had a well-fitted $sech^2$-shaped spectrum with an FWHM of 47 nm at 2086 nm and a temporal FWHM of 98 fs, derived from the autocorrelation trace. Assuming a $sech^2$-shaped temporal profile, the resulting time-bandwidth product (TBP) was 0.317, which is evidence for the generation of soliton pulses with a nearly Fourier-limited duration, as expected from the almost perfect fits both in the spectral and in the temporal domains.

The shortest pulses were achieved by reducing the output coupling to 0.5% at the expense of the average power. After extra-cavity linear chirp compensation with a 3-mm-thick polycrystalline ZnS plate (GDD = 465 fs^2 at 2.08 μm), the pulses were compressed from 66 to 58 fs (eight optical cycles). The average output power amounted to 114 mW for an absorbed pump power of 2.19 W. The ML laser spectrum with a central wavelength of 2076 nm exhibited a significant spectral broadening compared to operation with 1.5% and 3% OC, owing to relatively strong SPM originating from the Tm:$(Lu,Sc)_2O_3$ ceramic, as shown in Figure 6(a). The on-axis intracavity peak intensity on the ceramic sample reached 292 GW/cm^2. The pulse duration, which was deconvolved from the measured fringe-resolved autocorrelation trace after compression [see Figure 6(b)], is 20.8% longer than the Fourier-transform limited value of the measured spectrum. We attribute the asymmetric spectral profiles (deviation from the ideal $sech^2$-shaped spectral profile) to the unmanageable intracavity GDD at the long-wave spectral wing, that is, at wavelengths higher than 2.15 μm, and the non-optimized reflection bands of individual cavity mirrors (cf. Figures 4(a) and 6(a)).

The stability in the ML regime of the laser was confirmed by measurements with a radio frequency (RF) spectrum analyser in two frequency span ranges. The recorded fundamental beat note at 82.94 MHz exhibited a high signal-to-noise ratio (SNR) of more than 75 dBc (see Figure 7(a)). The uniform harmonic beat notes in the 1-GHz frequency span (see Figure 7(b)) are evidence for stable steady-state ML operation without any *Q*-switching and/or multi-pulsing instabilities.

4. Conclusion

In conclusion, we demonstrated average power scaling of an SWCNT-SA ML 'mixed' Tm:$(Lu,Sc)_2O_3$ ceramic laser maintaining the sub-100-fs regime near 2 μm. Pulses as short as 58 fs were generated at 2076 nm with an average power of 114 mW and a pulse repetition rate of approximately

82.9 MHz. A maximum average output power as high as 486 mW was directly obtained from the ML laser at 2086 nm for a pulse duration of 98 fs, with a conversion efficiency of 22.3%. This represents the highest average output power and conversion efficiency ever reported from any sub-100-fs ML Tm laser. Given the imperfect design of the cavity mirrors, shorter pulse durations would be possible after optimizing the reflection bands of the cavity mirrors, as well as by fine control of the total intracavity GDD over the full spectral bandwidth of the ML laser.

Acknowledgements

This work was partly supported by the National Natural Science Foundation of China (NSFC) (52032009, 61975208, 62075090, 51761135115, 61575199, 61850410533, and 52072351); Deutsche Forschungsgemeinschaft (PE 607/ 14-1); Sino-German Scientist Cooperation and Exchanges Mobility Program (M-0040); Natural Science Foundation of Jiangsu Province (BK20190104); National Research Foundation of Korea (2020R1A4A2002828); CAS Key Laboratory of Optoelectronic Materials Chemistry and Physics, FJIRSM CAS (2008DP173016); Foundation of the President of China Academy of Engineering Physics (YZJJLX2018005); State Key Laboratory of Crystal Materials (SKLCM), SDU (KF2001). Yongguang Zhao acknowledges financial support from the Alexander von Humboldt Foundation through a Humboldt fellowship.

References

1. V. Petrov, Prog. Quantum Electron. **42**, 1 (2015).
2. V. O. Smolski, H. Yang, S. D. Gorelov, P. G. Schunemann, and K. L. Vodopyanov, Opt. Lett. **41**, 1388 (2016).
3. T. Fuji, N. Ishii, C. Y. Teisset, X. Gu, T. Metzger, A. Baltuska, N. Forget, D. Kaplan, A. Galvanauskas, and F. Krausz, Opt. Lett. **31**, 1103 (2006).
4. T. Popmintchev, M. Chen, D. Popmintchev, P. Arpin, S. Brown, S. Ališauskas, G. Andriukaitis, T. Balciunas, O. D. Mücke, A. Pugzlys, A. Baltuška, B. Shim, S. E. Schrauth, A. Gaeta, C. Hernández-García, L. Plaja, A. Becker, A. Jaron-Becker, M. M. Murnane, and H. C. Kapteyn, Science **336**, 1287 (2012).
5. R. R. Gattass and E. Mazur, Nat. Photonics **2**, 219 (2008).
6. A. A. Lagatsky, Z. Sun, T. S. Kulmala, R. S. Sundaram, S. Milana, F. Torrisi, O. L. Antipov, Y. Lee, J. H. Ahn, C. T. A. Brown, W. Sibbett, and A. C. Ferrari, Appl. Phys. Lett. **102**, 013113 (2013).
7. A. A. Lagatsky, O. L. Antipov, and W. Sibbett, Opt. Express **20**, 19349 (2012).
8. M. Tokurakawa, E. Fujita, and C. Kränkel, Opt. Lett. **42**, 3185 (2017).
9. C. Kränkel, IEEE J. Sel. Top. Quantum Electron. **21**, 1602013 (2015).
10. N. K. Stevenson, C. T. A. Brown, J. M. Hopkins, M. D. Dawson, and A. A. Lagatsky, Opt. Express **27**, 11103 (2019).
11. N. K. Stevenson, C. T. A. Brown, J. M. Hopkins, M. D. Dawson, C. Kränkel, and A. A. Lagatsky, Opt. Lett. **43**, 1287 (2018).
12. J. Vetrovec, D. M. Filgas, C. A. Smith, D. A. Copeland, A. S. Litt, E. Briscoe, and E. Schirmer, Proc. SPIE **10511**, 1051103 (2018).
13. W. Jing, P. Loiko, J. M. Serres, Y. Wang, E. Vilejshikova, M. Aguiló, F. Díaz, U. Griebner, H. Huang, V. Petrov, and X. Mateos, Opt. Mater. Express **7**, 4192 (2017).
14. Z. Y. Zhou, X. F. Guan, X. X. Huang, B. Xu, H. Y. Xu, Z. P. Cai, X. D. Xu, P. Liu, D. Z. Li, J. Zhang, and J. Xu, Opt. Lett. **42**, 3781 (2017).
15. Y. Wang, W. Jing, P. Loiko, Y. Zhao, H. Huang, X. Mateos, S. Suomalainen, A. Härkönen, M. Guina, U. Griebner, and V. Petrov, Opt. Express **26**, 10299 (2018).
16. Y. Zhao, L. Wang, Y. Wang, J. Zhang, P. Liu, X. Xu, Y. Liu, D. Shen, J. E. Bae, T. G. Park, F. Rotermund, X. Mateos, P. Loiko, Z. Wang, X. Xu, J. Xu, M. Mero, U. Griebner, V. Petrov, and W. Chen, Opt. Lett. **45**, 459 (2020).
17. Y. Zhao, L. Wang, W. Chen, Z. Pan, Y. Wang, P. Liu, X. Xu, Y. Liu, D. Shen, J. Zhang, M. Guina, X. Mateos, P. Loiko, Z. Wang, X. Xu, J. Xu, M. Mero, U. Griebner, and V. Petrov, Appl. Opt. **59**, 10493 (2020).
18. Y. C. Wang, W. D. Chen, M. Mero, L. Z. Zhang, H. F. Lin, Z. B. Lin, G. Zhang, F. Rotermund, Y. J. Cho, P. Loiko, X. Mateos, U. Griebner, and V. Petrov, Opt. Lett. **42**, 3076 (2017).
19. L. Wang, W. Chen, Y. Zhao, Y. Wang, Z. Pan, H. Lin, G. Zhang, L. Zhang, Z. Lin, and J. Bae, Opt. Lett. **45**, 6142 (2020).
20. Y. Wang, Y. Zhao, Z. Pan, J. E. Bae, S. Y. Choi, F. Rotermund, P. Loiko, J. M. Serres, X. Mateos, H. Yu, H. Zhang, M. Mero, U. Griebner, and V. Petrov, Opt. Lett. **43**, 4268 (2018).
21. A. Suzuki, C. Kränkel, and M. Tokurakawa, Appl. Phys. Express **13**, 052007 (2020).
22. Z. Pan, Y. Wang, Y. Zhao, H. Yuan, X. Dai, H. Cai, J. E. Bae, S. Y. Choi, F. Rotermund, X. Mateos, J. M. Serres, P. Loiko, U. Griebner, and V. Petrov, Photon. Res. **6**, 800 (2018).
23. E. Ugolotti, A. Schmidt, V. Petrov, J. W. Kim, D. I. Yeom, F. Rotermund, S. Bae, B. H. Hong, A. Agnesi, C. Fiebig, G. Erbert, X. Mateos, M. Aguilo, F. Diaz, and U. Griebner, Appl. Phys. Lett. **101**, 161112 (2012).
24. W. B. Cho, J. H. Yim, S. Y. Choi, S. Lee, A. Schmidt, G. Steinmeyer, U. Griebner, V. Petrov, D. I. Yeom, K. Kim, and F. Rotermund, Adv. Funct. Mater. **20**, 1937 (2010).
25. J. A. Caird, S. A. Payne, P. Staber, A. Ramponi, L. Chase, and W. F. Krupke, IEEE J. Quantum. Electron. **24**, 1077 (1988).
26. A. Schmidt, S. Y. Choi, D. I. Yeom, F. Rotermund, X. Mateos, M. Segura, F. Diaz, V. Petrov, and U. Griebner, Appl. Phys. Express **5**, 092704 (2012).
27. F. Kartner, I. Jung, and U. Keller, IEEE J. Sel. Top. Quantum Electron. **2**, 540 (1996).
28. D. E. Zelmon, J. M. Northridge, N. D. Haynes, D. Perlov, and K. Petermann, Appl. Opt. **52**, 3824 (2013).